NIPES

Journal of Materials Engineering, Structures and Computation

Journal homepage: www.nipesjournals.org.ng

Effects of Welding Current Gas Flow Rate and Welding Voltage on Thermal Conductivity Using Response Surface Methodology

Martins Ufuoma Eki[a], Joseph Achebo[b] and Kessington Obahiagbon.[c]

[a]Department of Mechanical Engineering. Federal University of Petroleum Resources Effurun, Delta State, Nigeria.
[b] Department of Production Engineering. University of Benin City, Edo State, Nigeria.
[c] Department of Chemical Engineering. University of Benin, Edo State, Nigeria.
eki.martins@fupre.edu.ng [a] josephachebo@yahoo.co.uk[b] kess.obahiagbon@uniben.edu[ab]

ARTICLE INFORMATION

Article history:
Received 24 December 2022
Revised 25 December 2022
Accepted 27 December 2022
Available online 11 January 2023

Keywords:
Conductivity, Voltage, Welding, Flow rate, Current

*https://doi.org/*10.5281/zenodo.7525700

ABSTRACT

In this experimental work, the effects of welding current, gas flow rate and welding voltage on thermal conductivity using RSM were studied, and the use of numerical models to further improve understanding of welding properties is of great importance to the welding researchers. RSM is a very significant technique applied in the Manufacturing, Oil and Gas, Metallurgical and Materials industries that employ mathematical and artificial intelligent methods. This paper is on Tungsten inert gas process parameters. The main input variables considered are welding voltage, welding current and gas flow rate. The response parameter is thermal conductivity. The statistical design of the experiment was carried out 20 times with 5 weld specimens per experiment, using the central composite design matrix. The response was measured and recorded. Gas Flow Rate of 10Lit/min, Voltage of 9Volts, and Current of 160Amp results in thermal conductivity of 42.96123w/m.

1. Introduction

According to Khanna [1], welding is more economical, convenient and less susceptible to failure or corrosion as compared to other joining processes. Welding is advantageous compared to other manufacturing processes of welding developed.

Reactions of kinetics that exist between slag and metal can be inspected by measuring the viscosity of liquid constantly. Kaptay [2] said that the viscosity of liquid metals and alloys is one of the technologically important transport properties needed to develop and optimize metallurgical technologies. According to Aoki et al. [3] the gas tungsten arc welding (GTAW) process is based on the electric arc established between a non-consumable electrode of tungsten and the work-pieces to be joined. The electric arc generates part of the heat that is added to the workpiece for the formation and promotion of the weld pool, which is prevented from contamination of air by a stream of inert gas (He or Ar) or gases mixed together. This is also known as tungsten inert gas (TIG), though it uses small amounts of inert gases such as nitrogen or hydrogen as shielding gas mixture.

Autogenous GTA welding (filler metal absence) utilized sections with thin edge-square (2mm), thicker sections require V and X-type preparation and require the addition of filler metal. In this case, the addition of filler metal is required. Pieces of carbon and low alloy steels including thin parts of stainless steel, titanium alloys, magnesium, and aluminum are extensively utilized in this process of metal joining.

GTA welding has heat input that does not rely on the filler material rate. Therefore, this process of welding permits specific control of heat addition and high-quality weld manufacture, free of spatter and low disruption. The consumable electrode has a lower economic benefit when compared to other methods of arc welding because it is responsive to a windy environment, there is difficulty in protecting the weld pool and it has a lesser deposition rate. Besides, it shows lesser tolerance to contaminants on filler or parent metals. Norrish [4] stated that the autogenous process is readily used in robotics, although special techniques are required when it is essential to add filler metal to the weld pool. Constant current types with drooping volt-ampere static curves are GTA welding power sources. Presently, transistorized lightweight direct current power sources are utilized because of their ability and stability compared to old thyristor-controlled units. The A/C current is restored and then converted into a high frequency when compared to the main supply inverter in the rectifier inverter inward A/C current power source. Appropriate for welding in the transformer, high voltage, A/C current, changed into low voltage A/C current and rectified afterward. The welding torch holds the non-consumable electrode, making sure of the transfer of current to the electrode and the flow of shielding gas to the weld pool. Uninterrupted operation between 200A and 500A are water cooled in the Torch's welding regime. Pure tungsten or tungsten alloys are parts of the non-consumable electrode. Lower service lifespan, susceptibility to contamination and exhibition of higher tip wear and tear than alloyed electrode but can be utilized with DC. Magnesium alloys aluminium can be welded by this electrode.

Non-consumable electrodes are made up of pure tungsten or of tungsten alloys. According to Watanabe [5], GTAW is regarded as a high-quality process for welding thin metals using low travel speed and low electrode deposition rate, requiring highly skilled personnel in manual welding.

1.1. Welding Process Parameters

The relevant variables for the GTAW process are current, voltage, filler metals, electrode vertex angle, welding speed, shielding gases, and arc length. Welding speed, weld bead shape and quality of weld joint is directly affected by current. According to Shirali and Mills [6], welding speed does not control the electromagnetic force and the arc pressure since they are dependent on the current. Reduction in the weld cross-sectional area is a result of an increase in the weld width (W) and depth (D) of penetration reduction, but the D/W ratio has a weak reliance on the speed of travel. The weld speed increase results in a reduction in the weld cross-sectional area and therefore, penetration depth (D) and weld width (W) also reduce but the D/W ratio has a weak reliance on travel speed. The mechanism involved in the weld pool formation is not influenced by travel speed, it only has an effect on melted material volume according to the result. Ordinarily, material type, plate thickness, and current influence welding speed between 100 to 500mm/min. Most of the metals being welded utilized gases with 99.995% purity, although, titanium which is a reactive material needs less than 50 ppm. Filler metals are generally used for plate thickness above 2mm, having a chemical composition similar to that of the parent materials [6]. Automatic systems are usually added cold from the roll or a coil between 1.6 and 3.2mm, which is the filler metal diameter. Norrish [4] stated that this technique also tends to increase the risk of the undercut. In the automated GTA welding method to increase penetration depth very high current ($I > 300A$) may be utilized. The procedure becomes not stable above 500A when the defect is formed.

1.2. Tungsten Inert Gas (TIG)

Electricity is passed to the tungsten electrode for an electric arc to occur in the TIG welding process. The distance between the tip of the tungsten electrode and the workpiece surface will cause the flow of electrons which in turn produces arc and high heat to melt the metal.
Narang et al. [7] explained that a shielded atmosphere is required when utilizing tungsten contact with the electrode in TIG welding, which produces an arc making the metal to be molten. A higher frequency of Alternating Current or Direct Current is utilized to enable a stable and uninterrupted arc without contact with the electrode. The cleanest weld bead is the reason TIG welding becomes the technology preferred most. TIG welding variables were studied by researchers applying a Fuzzy logic controller for establishing the relationship between responses and input process variables this indicates that the method is satisfactory.
Eki et al. [8] said Aero- disperses poisonous particles, which can be hazardous to the respiratory system of welding practitioners are accompanied by TIG welding processes. They developed a near-optimal solution to reduce the fume concentration in TIG welding by systematically applying the genetic algorithm approach.
Assar et al. [9] investigated the effect of heat input of gas tungsten arc welding on the microstructure of mechanical properties of AZ91 magnesium alloy. The studies were performed by using, scanning electrons and an optical microscope equipped tensile test, energy dispersive X-Ray spectroscopy was applied to evaluate the mechanical properties. The results show, thickness moderately increases the melted zone, with heat reduction in tensile strength of welded samples observed compared to a base metal. It reduces with increased studying of fracture surface; the formation of cleavages was a prevalent fracture mechanism when carrying out the tensile test.

1.3. Parameter Selection

The factors that define the limits of the thickness of the wall that influence the surface finish quality are weld bead dimensions and shape. Wire feed, welding speed, arc voltage, and welding current are the four main variables. Four small-the better quality is the optimal weld pool geometry that is solved with the modified Taguchi methods. According to Tradia et al. [10] the optimal weld pool geometry has four smaller-the-better quality characteristics, i.e. the front height, front width, back height, and back width of the weld pool. The modified Taguchi method is selected to solve the optimal weld pool geometry with four smaller-the better quality. Dongjie et al. [11] did their research based on the three-parameter selection which is speed travel, arc length, and current. In studies on gap distance (arc gap) shielding gas flow rate, and welding speed, the Taguchi method was found to be an effective optimization tool, because it gave significant effects on the bead geometry.

1.4. Factorial Design

Gupta and Parmar [12] used the fractional factorial technique to develop mathematical models to predict the weld bead geometry and shape relationships for the SAW of micro-alloyed steel, the thickness ranging between 10mm and 16 mm. They carry out research on workpiece thickness, welding speed, nozzle-to-plate distance, open circuit voltage, width/reinforcement as affected by wire federate, width/penetration, dilution, reinforcement, weld width, and bead penetration. The result shows that with welding parameters, a different combination of interaction effects, and the prediction of the main effects, the factorial technique was suitable.

1.5. Linear regression

Yang et al. [13] developed linear regression equations for computing the weld features (melting rates, total fusion area, penetration, deposit area, bead height, and bead width) from SAW process variables (electrode extensions range, welding voltage, welding current, welding speed, and electrode diameter) using both positive and negative electrode polarity.19 mm thick ASTM A36 steel plate was the parent material used for the study. Regression equations were developed for each weld in both polarity conditions. They reveal that were suitable for computing numerous features of the SAW process.

2. Methodology

2.1 Research Design

This study is on TIG mild steel welds experiments, tests for mechanical properties, statistical and expert systems. It employed the scientific design of the experiment. The overall plan chose to integrate the different research components in a coherent and logical way so as to effectively address the study under review. This study is centered on the experimental study of TIG mild steel welds, employing scientific design of experiments, expert systems, statistical and mathematical models, and tests for mechanical properties.

2.2 Design of experiment

Experimentation is a very significant aspect of scientific study, which can be developed using computer software like design expert and Minitab. For proper polynomial approximation, an experimental design is employed to collect the data. There are different types of experimental designs which include Central Composite design, Taguchi, D-optimal design, Factorial design, and Latin Hyper Cube designs.

2.3 Identification of the range of input parameters

Welding voltage, gas flow rate, and welding current, in this work, are the key parameters considered Table 1 below shows the range of processes obtained from the literature.

2.4 Population

200 coupons of mild steel pieces 60 x 40 x10mm by measurement, were utilized for this experiment, which made use of 10 coupons welded to form 5 samples for each run, performed 20 times.

2.5 Method of Data Collection

Using the design expert software, the design matrix of the central composite design was developed. The experimental matrix is made up of the output and input variables. The central composite design matrix is shown in Table 2 below. The response recorded, from the welded specimen was applied as data.

2.6 Method of Data Analysis

Response surface methodology was employed to obtain and analyze the data.

2.7 Response Surface Methodology

The process of interest is very important to engineers. They search for conditions that are optimized. The values at which the response reaches their optimum and values of process input variables at which the response reaches their optimum. The maximum or minimum can be the optimum. Response Surface Methodology (RSM) can be defined as a set of statistical and mathematical technique, used for predicting and modeling input parameters, that the response of interest affect, with the purpose of response optimization.

2.8 Testing the adequacy of the models developed

The analysis of variance (ANOVA) was used to test the adequacy of the models developed. The statistical significance of the models developed and each term in the regression equation was examined using the sequential F-test, lack-of-fit test, and other adequacy measures (i.e., R^2, Adj- R~, Pred. R^2, and Adeq. Precision ratio) using the same software to obtain the best fit. The Prob.>F (sometimes called p-value) of the model and of each term in the model can be computed by means of ANOVA. If the Prob.> F of the model and of each term in the model does not exceed the level of significance (say a = 0.05) then the model may be considered adequate within the confidence interval of (1 ─ a). The lack-of-fit test could be considered insignificant if the Prob.>F of the lack of fit exceeds the significance level.

3. Results and Discussion

3.1. Modelling and Optimization using RSM

200 coupons of mild steel pieces, 60 x 40 x10mm by measurement utilized for these experiments, which made use of 10 coupons welded to form 5 samples for each run, performed 20 times, each experimental made up of gas flow rate, voltage, and current. Response surface methodology uses computer software such as design expert to develop mathematical models and the steps taken to develop the models include the, lack of fit test, analysis of variance, goodness of fit sequential sum of squares, and model summary statistics.
As presented in Table 3, the calculation for the thermal conductivity responses was done in experimental data analysis of the sequential model sum of squares, for quadratic model suitability validation. As terms are added to the model fit, the accumulating improvement, Table 3, shows the sequential model sum of squares.
The model, selected as the best fit was the model that is not aliased, the additional terms are significant and the polynomial order is the highest, based on the sequential model sum of the square. Table 3 results indicate that cubic polynomial cannot be utilized because it was aliased.
In this analysis, the quadratic polynomial, justifying as best fit and suggested, is 2FL VS the quadratic in addition.

Significant lack of fit model, not suitable for prediction. The individual responses were tested and estimated with the lack of fit experimental data associated with underlying variation to be explained using the quadratic model, Results for computed lack of fit for thermal conductivity are presented below in Table 4. From the result of Table 4 quadratic polynomial was aliased model analysis, because a non-significant lack of fit was observed. The computed statistical model, based on model sources for thermal conductivity is shown in Table 5. From model fit statistics summary, indicates, for each computed model, the Predicted error sum of square (PRESS) Statistics, predicted r-squared, adjusted r- squared, the r-squared, and Standard deviation. The best model source optimal criteria for its definition; Relatively low PRESS, R-squared, low Standard deviation. The Quadratic Polynomial model was selected for this analysis, because, the cubic polynomial model was

suggested, based on Table 5 result. Figure 1 shows thermal conductivity against selected input variables (gas flow rate, voltage, and welding current) combined interactions. The above shows the optimal equation and that indicates the individual interaction effects.

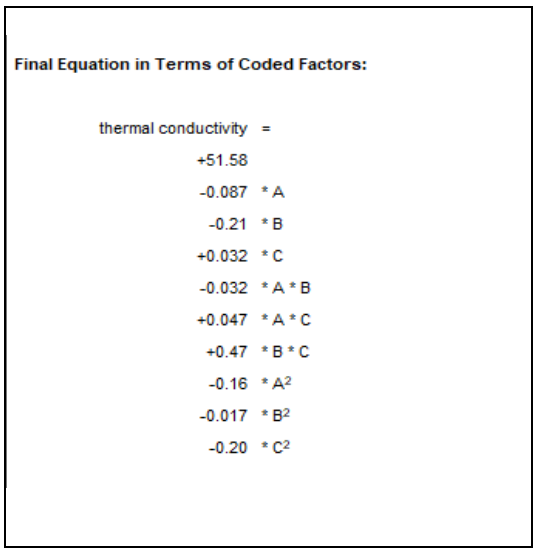

Figure 1. The optimal equation in terms of coded factors for minimizing thermal conductivity

The optimal equation which indicates the individual effects and combines interactions of the selected input variables (welding current, voltage and gas flow rate) against the thermal conductivity is presented based on the actual variables in Figure 2.

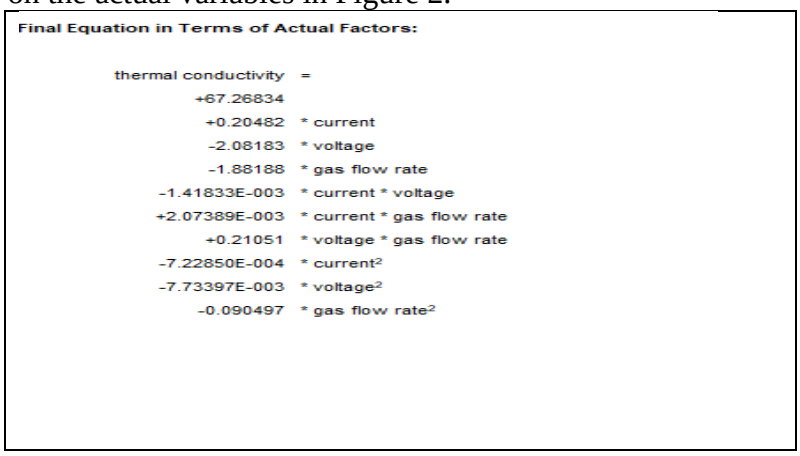

Figure 2. An optimal equation in terms of actual factors for minimizing thermal conductivity

The diagnostics case statistics which indicate the observed values of thermal conductivity and their predicted values are presented in Table 6 below. The diagnostics case statistics actually give insight into the model strength and the adequacy of the optimal second-order polynomial equation.

The suitability of the model must first be checked by an appropriate statistical analysis output, to accept any model.

To diagnose the statistical properties of the thermal conductivity response surface model, the normal probability plot of the residual is presented in Figure 3.

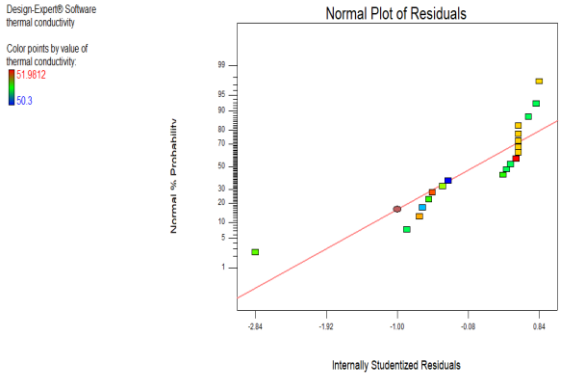

Figure 3. Normal probability plot of studentized residuals for thermal conductivity

Despite the slight scatter, of the points, it was observed that a straight line was followed. No specified pattern is likened to an "s-shape" curve. For better analysis, no transformation of the response data is required. To assess the normality of the calculated residual, a normal probability plot of residuals was employed. To ascertain, if the residuals (observed- predicted) follow a normal distribution, a normal probability plot of residuals which is the number of the standard deviation of actual values based on the predicted values was employed. An indication that the model developed is satisfactory and normally distributed is used to check. It is the most significant assumption for checking.

To detect the presence of mega patterns or expanding variance, a plot of residuals and the predicted was produced for the thermal conductivity which is shown in Figure 4.

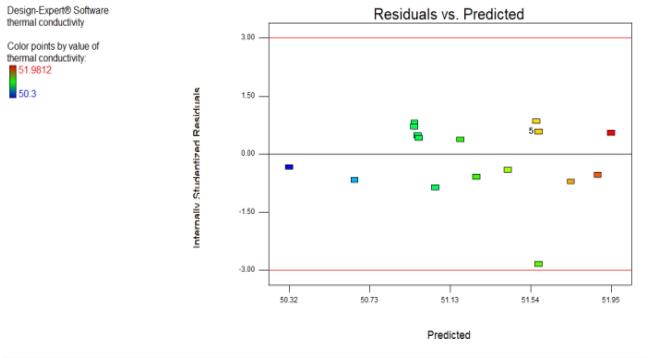

Figure 4. The plot of Residual vs Predicted thermal conductivity

The points are close to the line of fit as shown in the graph. For a group of values or a value to be detected, that is not easily detected by the model is actually able to predict most of the data point.

For thermal conductivity response as shown in Figure 5, the predicted values are plotted against the actual values

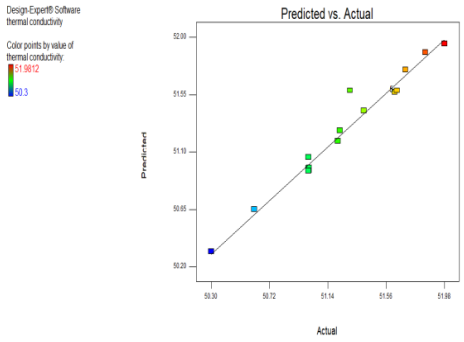

Figure 5. The plot of Predicted Vs Actual for the thermal conductivity response

To study the effects of current and voltage on thermal conductivity, the 3D surface plot presented in Figure 6 was generated as follows:

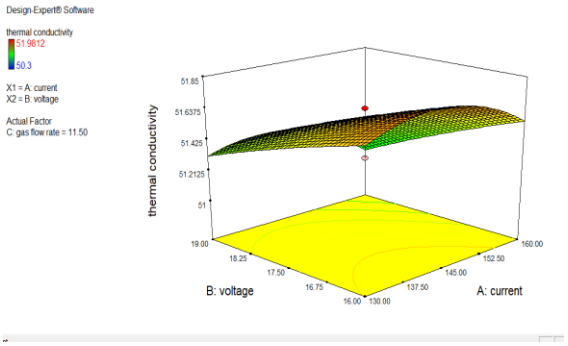

Figure 6. Effect of current and voltage on the thermal conductivity

To study the effects of current and gas flow rates on the thermal conductivity, the 3D surface plot presented in Figure 7 was generated as follows:

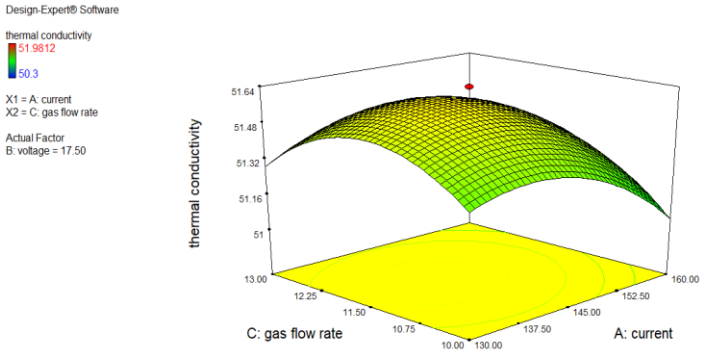

Figure 7. Effect of current and gas flow rate on the thermal conductivity

To study the effects of voltage and gas flow rate on the thermal conductivity, the 3D surface plot presented in figure 8was generated as follows:

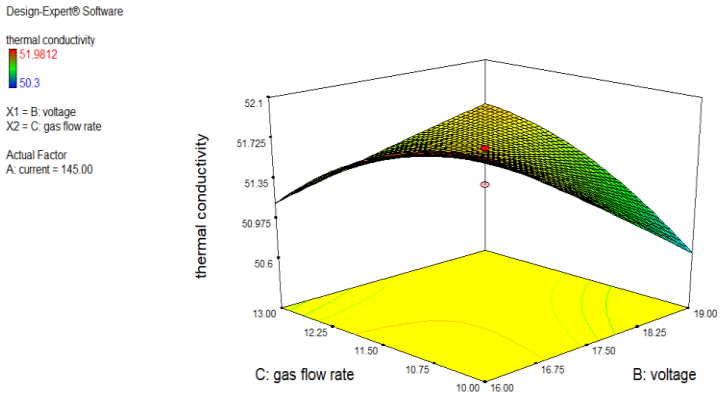

Figure 8. Effect of voltage and gas flow rate on the thermal conductivity

Design expert was used to minimize thermal conductivity. The optimum current, voltage, and gas flow rate, were determined simultaneously. The interphase of the numerical optimization thermal conductivity as the objective function is presented in Figure 9.

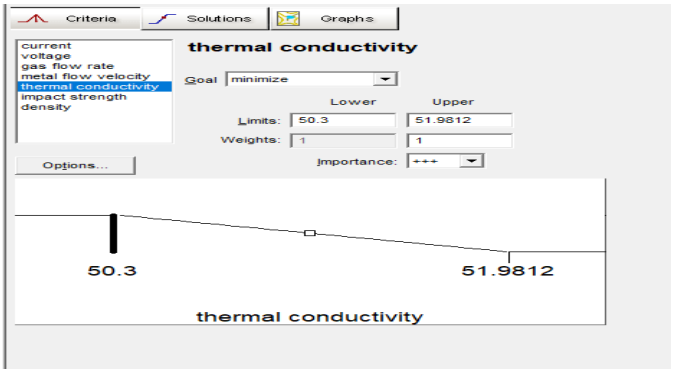

Figure 9. Interphase of a numerical optimization model for thermal conductivity

From the results of Table 7, it was observed that a current of 160amps, voltage of 19volts, and gas flow rate of 10lit/min will result in a welding process with the properties:

Thermal conductivity 50.32

This solution was selected by a design expert as the optimal solution with a desirability value of 98.6% as shown below in Table 7.

Finally, based on the solution, the contour plots showing the thermal conductivity variable against the optimized value of current and voltage are presented in Figure 10.

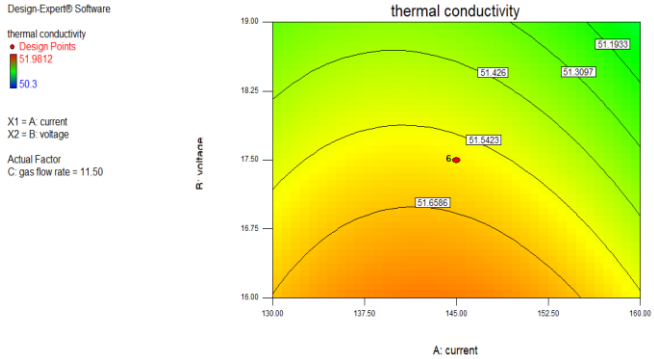

Figure 10. Contour plot of current and voltage predicting thermal conductivity

4. Conclusion

In this study, Response Surface Methodology has been applied in predicting the thermal conductivity, of TIG mild steel weld. The model considered was; current, voltage and gas flow rate as input variables, while the output was thermal conductivity. An appropriate experimental design and test samples were produced for this study.

Nomenclature

ANOVA	Analysis of Variance
DOE	Design of Experiment
TIG	Gas Tungsten Arc Welding
GFR	Gas Flow Rate
MFV	Metal Flow Velocity
P –Value	Probability Value
P >F	P >F Sometimes called P –Value
PRESS	Predicted Error Sum of Square Statistics
Q	Quadratic Polynomial Model
R^2	Coefficient of Determination
RSM	Response Surface Methodology
Std	Standard deviation
3D	Three dimensions

References

[1] O.P. Khanna. (1999) “Material Science and Metallurgy”, DhanpatRal Publication Ltd, New Delhi.
[2] G. Kaptay. (2005) A Unified Equation for The Viscosity of Pure Liquid Metals. Z. Metalld, 96 (1), pp, 1-8.
[3] A. Aoki, M. Takeichi, M. Seto, S.Yamaguchi. (2004), Development of GTAW robot system for aluminium frame, IIW Doc Vol. 12 pp1814-04
[4] J.Norrish.(1992) Advanced welding processes, Advanced welding processes. Springer Science & Business Media.
[5] H.Watanabe, Y.Butsusaki, T. Nagashima (2004), Development of ultra-narrow gap hot wire GTA welding process, IIW Doc. Vol. 12. pp1810-04.
[6] A.Shirali, and K. Mills (1993).Effect of welding parameters on penetration in GTA welds. Welding Journal Vol. 72(7), pp. 347s – 353s.
[7] H.K.Narang, U.P.Singh,M.M.Mahapatra P.K. Jha (2011). Prediction of the Weld Pool Geometry of TIG Arc Welding by Using Fuzzy Logic Controller. International Journal of Engineering, Science and Technology, Vol.3(9), pp77-85.
[8] M.U. Eki, J.I Achebo, A.Ozigagun (2020). Analysis and optimization of safe welding fumes in tig welding, World Journal of Engineering Research and Technology Vol. 6 (4), pp 288-297
[9] B.Assar., N.Bani Mostafa Arab,I.Khoubrou.(2021). Effect of heat input of TIG repair welding on microstructure and mechanical properties of cast AZ91 magnesium alloy. Welding in the World Vol.65(6), pp1131 – 1143
[10] A.Tradia, F.Roger, E. Guyot, (2010). Optimal parameter for pulsed gas tungsten arc welding in partially and fully penetrated weld pools. International Journal of Thermal Sciences, Vol.49(7), pp1197-1208.
[11] Li, D., Lu, S., Dong, W., Li, D., & Li, Y. (2012). Study of the law between the weld pool shape variations with the welding parameters under two TIG processes. Journal of Materials Processing Technology. Vol. 212(1), pp128-136.
[12] V.K. Gupta, and R.S. Parmar,.(1989) Fractional Factorial Technique To Predict Dimensions Of The Weld Bead In Automatic Submerged Arc Welding, Ie(I) Journal-Mc, Vol. 70, Nov. Pp.67-75Kaptay, G. (2005) A Unified Equation For The Viscosity of Pure Liquid Metals. Z. Metalld. Vol. 96 (1), pp, 1-8.
[13] L. J. Yang, M.J.Bibby, R. S. Chandel, (1993) Linear Regression Equations For Modelling The Submerged-Arc Welding Process, J. Of Materials Processing Technology, Vol. 39(1-2), Pp. 33-42.

Appendix

Table 1. Process parameters and their levels

Parameters	Unit	Symbol	Coded value Low(-1)	Coded value High(+1)
Current	Amp	A	130	160
Gas flow rate	Lit/min	F	10	13
Voltage	Volt	V	16	19

Table 2. Experimental results

Run	I (Amp)	V (Volt)	GFR (Lit/min)	Thermal Conductivity, (W/m.^{o}C)
1	130	16	10	51.9812
2	140	17	11	51.2275
3	150	18	12	51.4845
4	160	19	13	51.9553
5	130	16	11	51.4950
6	140	17	12	51.6385
7	150	18	13	51.3844
8	160	19	10	51.7782
9	130	16	12	51.2133
10	140	17	13	51. 5992
11	150	18	10	51.3008
12	160	19	11	51.6304
13	130	16	13	51. 9628
14	140	17	10	51. 4996
15	150	18	11	51.2114
16	160	19	12	51.3411
17	130	19	13	51.6222
18	140	18	10	51.8420
19	150	17	11	51.7318
20	160	16	12	51.0043

Table 3. Sequential model sum of square for thermal conductivity

Source	Sum of Squares	df	Mean Square	F Value	p-value Prob > F	
Mean vs Total	52674.38	1	52674.38			
Linear vs Mean	0.70	3	0.23	1.31	0.3055	
2FI vs Linear	1.82	3	0.61	7.78	0.0032	
Quadratic vs 2FI	0.90	3	0.30	25.35	< 0.0001	Suggested
Cubic vs Quadratic	0.022	4	5.508E-003	0.34	0.8389	Aliased
Residual	0.096	6	0.016			
Total	52677.91	20	2633.90			

Table 4. Lack of fit test for thermal conductivity

Source	Sum of Squares	df	Mean Square	F Value	p-value Prob > F	
Linear	2.74	11	0.25	13.04	0.0054	
2FI	0.92	8	0.11	6.01	0.0319	
Quadratic	0.022	5	4.474E-003	0.23	0.9314	Suggested
Cubic	3.407E-004	1	3.407E-004	0.018	0.8990	Aliased
Pure Error	0.095	5	0.019			

Table 5. Model summary statisticsfor thermal conductivity

Source	Std. Dev.	R-Squared	Adjusted R-Squared	Predicted R-Squared	PRESS	
Linear	0.42	0.1972	0.0467	-0.3878	4.90	
2FI	0.28	0.7128	0.5802	0.3689	2.23	
Quadratic	0.11	0.9666	0.9366	0.9108	0.32	Suggested
Cubic	0.13	0.9729	0.9141	0.9398	0.21	Aliased

Table 6. Diagnostics case statistics report for thermal conductivity

Standard Order	Actual Value	Predicted Value	Residual	Leverage	Internally Studentized Residual	Externally Studentized Residual	Influence on Fitted Value DFFITS	Cook's Distance	Run Order
1	51.98	51.95	0.034	0.670	0.542	0.522	0.744	0.060	14
2	51.70	51.74	-0.044	0.670	-0.712	-0.693	-0.987	0.103	10
3	50.61	50.65	-0.042	0.670	-0.671	-0.651	-0.927	0.091	12
4	50.30	50.32	-0.021	0.670	-0.340	-0.325	-0.463	0.023	11
5	51.00	50.97	0.029	0.670	0.473	0.453	0.646	0.045	4
6	51.00	50.95	0.050	0.670	0.803	0.788	1.122	0.131	13
7	51.62	51.57	0.053	0.670	0.844	0.831	1.183	0.144	17
8	51.40	51.43	-0.026	0.670	-0.410	-0.392	-0.559	0.034	7
9	51.23	51.27	-0.040	0.607	-0.589	-0.569	-0.708	0.054	16
10	51.00	50.98	0.028	0.607	0.418	0.400	0.497	0.027	1
11	51.84	51.88	-0.037	0.607	-0.545	-0.524	-0.652	0.046	6
12	51.21	51.19	0.025	0.607	0.373	0.356	0.443	0.022	8
13	51.00	50.95	0.048	0.607	0.702	0.683	0.850	0.076	3
14	51.00	51.06	-0.059	0.607	-0.874	-0.862	-1.072	0.118	9
15	51.64	51.58	0.057	0.166	0.573	0.552	0.247	0.007	5
16	51.64	51.58	0.057	0.166	0.573	0.552	0.247	0.007	19
17	51.64	51.58	0.057	0.166	0.573	0.552	0.247	0.007	18
18	51.64	51.58	0.057	0.166	0.573	0.552	0.247	0.007	15
19	51.30	51.58	-0.28	0.166	-2.842	** -6.15	* -2.75	0.161	2
20	51.64	51.58	0.057	0.166	0.573	0.552	0.247	0.007	20

Table 7. Optimal solutions of numerical model

Number	Current	Voltage	Gas flow rate	Thermal conductivity	Desirability	
1	160.00	19.00	10.00	50.3217	0.986	Selected
2	160.00	19.00	10.04	50.346	0.933	
3	160.00	19.00	10.06	50.3616	0.878	
4	160.00	19.00	10.08	50.3709	0.779	
5	160.00	18.91	10.00	50.3636	0.776	
6	159.69	18.93	10.00	50.3652	0.772	